Genetic inactivation of *Semaphorin 3C* protects mice from kidney tissue damage upon injury.

Anxiang Cai[1]*, Guanyu Ye[1]*, Sandrine Placier[1], Perrine Frère[1], Brigitte Surin[1], Sophie Vandermeersch[1], Raphael Kormann[1], Xu-Dubois YC[1], Magali Genest[1], Morgane Lannoy[1], Christos E. Chadjichristos[1], Jean-Claude Dussaule[1], Peter J. Scambler[2], Christos Chatziantoniou[1] and Amélie Calmont[1]

[1] INSERM UMRS 1155, Kidney Research Centre, 4 rue de la Chine, 75020 Paris, France

[2] UCL Great Ormond Street Institute of Child Health, 30 Guilford Street, London WC1N 1EH, UK

* contributed equally

Correspondence to:

Dr Amélie Calmont

INSERM UMRS 1155, Kidney Research Centre, Tenon Hospital, 4 rue de la Chine, 75020 Paris, France.

Email: amelie.calmont@inserm.fr;

Phone: +33156018375

Running Headline: SEMA3C deleterious function in AKI

Abstract

Elucidating the deleterious pathways that govern acute kidney injury (AKI) initiation and extension is an important goal, as such knowledge can help guide the development of therapeutic interventions for the treatment of this global health problem. We found that the class III semaphorin SEMA3C was ectopically upregulated, de novo excreted and secreted upon kidney injury and hypothesised that it could play an active role in the aetiology of the disease. We genetically abrogated *Sema3c* during AKI progression and analysed subsequent renal morphological and functional defects in two well-characterised models of AKI, the ischemia/reperfusion and the Folic Acid nephrotoxicity. We found that lack of SEMA3C ameliorated tissue injury and renal function in AKI-induced nephropathy and protected the kidney against increased tissue oedema, increased neutrophil infiltration and altered blood flow. We also employed intravital microscopy combined with Evans Blue dye extravasation and primary culture of magnetically-sorted peritubular endothelial cells to identify an unrecognised role for SEMA3C in promoting vascular permeability. Our study provides an improved mechanistic understanding of the disease and the first evidence for the role of SEMA3C in kidney disease. Our analysis embraces the complexity of signalling events that promote AKI progression and emphasises the role of vascular permeability as a significant underlying cause of the disease.

Keywords: Genetically altered and transgenic models, Vascular permeability, Neuropilin 1, VEGF, Acute Kidney Injury, Class 3 semaphorin

Translational Statement

AKI is a common clinical condition associated with high risks of mortality and subsequent progression to CKD. Emerging evidence has proved the pivotal role of endothelial dysfunction in the aetiology of AKI. Our studies on a ligand-specific mouse suggest that SEMA3C, a protein involved in axon pathfinding and cardiovascular development, mediates damaging functions in AKI. We identified an unrecognised role for SEMA3C in vascular permeability and studied how this could translate into tissue oedema, neutrophil infiltration and altered blood flow. Our work, via deepening the understanding of AKI pathophysiology, could guide the development of therapeutic interventions for this intractable disease.

Introduction

Acute Kidney Injury (AKI) represents a severe health burden impacting about 13.3 million patients annually for a global death toll of 1.7 million[1]. Even if followed by renal function recovery, AKI is a major risk factor for the subsequent development of chronic kidney disease (CKD) and end-stage renal disease; a process known as AKI to CKD transition [2]. Accumulating evidence has revealed that endothelial dysfunction plays a key role in the initiation, extension and maintenance of AKI[3]. Dysregulation of pro-angiogenic factors and unsolved capillary hyperpermeability contribute to microvascular hypoperfusion, oedema, hypoxia and inflammation in AKI[4, 5]. These processes not only aggravate the initial injury but have long-term effects on renal function and repair phase, predisposing to renal fibrosis and CKD.

SEMA3C is an 85 kDa glycoprotein that belongs to the large family of semaphorins initially identified for their involvement in axon pathfinding[6]. Semaphorins exist primarily as membrane-bound proteins with the exception of class III semaphorins which are secreted as soluble molecules[7]. We and others have shown that embryos deficient for *Sema3c* presented with severe kidney and cardiovascular abnormalities[8, 9]. SEMA3C also controls the development of novel and aberrant vasculature, including cancer angiogenesis [10] and vascularisation within the degenerate human intervertebral disc [11]. SEMA3C acts via receptor complexes which include ligand-binding subunit Neuropilin 1 (NRP1) or Neuropilin 2 (NRP2) and a coreceptor consisting of one of four class plexin proteins[12].

In this study, we investigated the critical pathophysiological role played by SEMA3C in two well-characterised models of AKI, the ischemia/reperfusion (IR) and the Folic Acid (FA) nephrotoxicity. We used a genetic approach to abrogate *Sema3c* during AKI progression and analysed subsequent renal structural and functional defects. These studies revealed that lack of SEMA3C reduced AKI-induced nephropathy resulting in decreased kidney tissue damage and neutrophil infiltration. Our work provides the first evidence that ectopic upregulation of SEMA3C in the context of AKI is critical in the progression of the disease. It also identifies SEMA3C as a

key mediator of kidney microvascular permeability which could promote kidney injury progression in AKI.

Methods and Materials

Mouse strains

We used the *Sema3C*$^{flox/flox}$ (MGI:107557)[8], *Sema3C*$^{+/-}$ and *CAGGCre-ERTM* (MGI:2182767)[13] alleles for breeding appropriate animals for the experimental study. Generation of the *Sema3C*$^{+/-}$ allele was obtained by breeding *Sema3C*$^{flox/flox}$ with germline beta-actin-CRE (MGI: 2176050). *Sema3C*$^{-/-}$ embryos presented with the well-characterised renal and cardiac defects (Supplemental Figure 5). *Sema3c* conditional mutants (FA-*Sema3c* conds : *CAGGCre-ERTM;Sema3C*$^{flox/-}$) and wt littermate controls (FA-CTR: *Sema3c*$^{flox/+}$ or *Sema3c*$^{flox/flox}$) were treated with Tamoxifen (1 mg/40 g body weight) for 5 consecutive days and then subjected to a single intraperitoneal dose of FA (FA-treated animals) or vehicle (Sham animals). Successful *Sema3C* deletion was demonstrated by recombination PCR and by the reduction of SEMA3C induction upon FA treatment (Supplemental Figure 2). Mice were maintained on a mixed genetic background consisting of C57BL/6J and CD1. Genotyping primers are *Sema3C* Flox Forw 5'- GAATCTGGCAAAGGACGATG-3', *Sema3C* Flox Rev 5'- GACCACTGGGCTTGAGAGAG-3', *Sema3C* Null 5'-AAGGCGCATAACGATACCAC-3', CRE Forw 5'-TGGAAAATGCTTCTGTCCGTTTGC-3' and CRE Rev 5'-AACGAACCTGGTCGAAATCAGTG-3'. The exact number of samples (n) is listed in Figure Legends.

Kidney acute injury models

For Ischemia Reperfusion (IR), 8-week old males of the designated genotype were anesthetised (ketamine/xylazine, 100 and 10mg/Kg i.p.) and subjected to right kidney nephrectomy [14]. Buprenorphine was used (0.05mg/Kg) as analgesic drug. Right kidneys (or contralateral kidneys) were used as controls for Western Blots and IF. The left renal artery was clamped for 30 minutes at 37°C followed by 48 hours of reperfusion. At this time, blood samples and kidney tissues were collected for further analysis. Briefly, and in agreement with the 3R principle, kidneys were cut in 4 separate pieces to enable 1) cryosectioning, 2) paraffin embedding, 3) RNA extraction and 4) protein extraction. Folic Acid (FA) (240mg/Kg) in vehicle (0.3M $NaHCO_3$) or vehicle only, was administered by intraperitoneal injection. As expected, a single FA injection triggers reliable nephrotoxicity as assessed by histology analysis and abnormal kidney function and was associated with a morbidity of <5% for the experimental period [15], irrespective of the mouse genotype. Forty eight hours post FA injection, blood samples and kidney tissues were collected as described above. In some cases, a microangiography was performed by systemic injection of 2000 kDa FITC-

Dextran (100mg/10^{-3}Kg body weight) 24 hours post FA injection. Kidneys were collected 10 mins post injection and treated as described below. Animal work was conducted under animal licence C75-20-01 (INSERM UMRS-1155) and Home Office Licence PPL70/7892 (UCL Great Ormond Street-Institute of Child Health, London, UK). Experimental procedure was approved by the French Ethic Committee APAFIS #11991.

Intravital microscopy

Intravital scanning was performed using an inverted Olympus IX83 microscope equipped with a 37°C heated chamber. Briefly, the left kidney of anesthetised wild type mice was exposed by flank incision and gently pulled to allow insertion of a slit plate at the level of the renal artery and vein. This system allows the physical separation of the organ from the rest of the body. At that time, a total volume of 200µl composed of FITC-Albumin (100µg/g body weight; 50mg/ml stock solution, Sigma) mixed with either 0.9%NaCl (control, CTR), or 5µg recombinant mouse VEGF-A (VEGF-164, R&D Systems), or 5µg recombinant mouse SEMA3C (R&D Systems), was intravenously injected in the eye sinus. The animal was then flipped over to expose the kidney onto the microscope slide and image acquisition (1 image every 15 seconds for 30 minutes) could start instantaneously. Tilling acquisition was performed in widefield microscopy with IX83 and DP73 camera (Olympus).

In vivo permeability Miles assay

8-week old mice of the designated genotype were anesthetised and subjected to left renal artery clamping for 30 minutes at 37°C followed by 24 hours of reperfusion. At that time, retro-orbital injection (10µl/g of body weight) of Evans Blue dye (5mg/ml dissolved in 0.9% NaCl) was performed. 35 minutes post injection; anesthetised animals were thoroughly perfused with 0.9%NaCl via the left ventricle to remove all blood from the vasculature. Perfused kidneys were extracted, weighed and incubated in 100% Formamide overnight at 56°C. Extracted dye concentration was measured using a spectrophotometer at 600nm and the value obtained was reported as $OD_{600}/10^{-3}$ Kg of tissue. In this modified Mile's assay model the right contralateral kidney is used as an internal control. Intradermic injection (50µl) of recombinant mouse SEMA3C (2µg), mouse SEMA3A (2µg) and mouse VEGF-A (0.5µg) (R&D Systems) was performed on anesthetised wildtype mice kept on a 37°C heated waterbed at all time. The appearance of a blue spot was monitored, photographed and quantified 30 mins post injection as described above.

In situ hybridisation (ISH), Immunolabelling and Coloration

In situ hybridisation was carried out on 10-µm paraffin section based on methods described previously [8]. A digoxigenin-labelled probe from a mouse *Sema3C* cDNA plasmid (gift of Jonathan Raper, University of Pennsylvania, Philadelphia, Pennsylvania, USA) was used. For immunolabelling, kidneys were fixed in 4% paraformaldehyde in PBS and processed as 10-µm frozen sections according to standard protocols. Briefly, sections were permeabilised in 0.5% Triton X-100 for 5mins, and incubated in blocking buffer for 1hr at room temperature (PBS/10% BSA/10% goat serum/0.1% Triton X-100) followed by primary antibody incubation in blocking buffer at 4°C overnight. For paraffin human biopsies, heat-induced antigen retrieval in Target Retrieval Solution Citrate pH 6 (Dako) was carried out after deparaffinisation and rehydration; sections were then blocked and processed as described above. All patients from Tenon's hospital provided informed consent to participate in the study. Either time-zero or protocol biopsies at 3 months in renal transplantation were used as controls. Primary antibodies are rabbit anti-SEMA3C (Abcam), goat anti-NRP1 and goat anti-NRP2 (R&D systems), rat anti-neutrophil NIMP-R14 (abcam), rat anti-Endomucin (Santa Cruz), mouse anti-CD34 (Euro Diagnostica), rabbit anti-MCM2 (Cell signalling), Rat anti-CD31 (BD Pharmingen), rabbit anti-SM22 α and rabbit anti cleaved caspase-3 (Abcam), and rat anti-Ki67 (Invitrogen). Secondaries were Alexa Fluor conjugated antibodies (Life Technologies and Jackson ImmunoResearch). Periodic Acid-Schiff (PAS) staining was used to semi-quantitatively score the degree of kidney injury by one blinded nephrologist specialised in anatomical pathology. Both tubular dilatation and necrosis (presence of tubular casts) were evaluated using the following scale: 0, no tubular damage; 1, damage in 1–25% of the tubules analysed; 2, damage in 26–50% of the tubules analysed; 3, damage in 51–75% of the tubules analysed; 4, damage in >76% of the tubules analysed, and the mean value was calculated for each mouse. Additional morphological features such as brush border integrity and thickness of the tubular epithelium was taken into consideration for establishing the definitive value. For neutrophil and cleaved caspase 3 staining, 3 fields of x10 magnification were quantified per specimen. Images were captured on a Zeiss Axoplan2 upright microscope and quantified with FIJI (ImageJ).

Isolation, culture and staining of peritubular capillary ECs from adult mouse kidneys

Primary peritubular capillary ECs were isolated from wildtype adult mouse using magnetic beads as previously described[16]. Briefly, kidneys were decapsulated, minced and digested in Collagenase (2mg/ml Collagenase Type I, Roche) at 37°C for 1 hour. Single cell suspension was then filtered

through a 100µm and a 40µm cell strainer (Fischer Scientists), centrifuged and resuspended in 1 ml isolation buffer (1X PBS, 0.5% BSA, 2mM EDTA, pH 7.4). Prior to isolation, anti-CD1 antibodies (BD Biosciences, #553370) were incubated with Dynabeads anti-rat IgG (Invitrogen) at 4°C overnight. Cell suspension was then magnetically labelled with beads-conjugated CD31 antibodies for 1hr at 4°C and isolated according to the manufacturer's instructions. Peritubular ECs were collected and cultured in endothelial cell growth medium (PromoCell, Germany, 10% FCS and 1% penicillin-streptomycin) on 1% gelatine pre-coated plates at 37°C. More than 86% of magnetically-sorted primary ECs were positive for EC markers CD31 and Endomucin (Figure 3B). For staining, ECs were fixed with either 4%PFA (15mins, room temperature) or 100% Methanol (10mins, -20°C) and processed as described above. For tube formation, Matrigel (Corning, NY, USA) was added in 24-well plate (200µl/well) and polymerized at 37°C for 45minutes. ECs were trypsinized at 37°C for 5 minutes, centrifuged and resuspended with endothelial cell medium containing none (control group), 300mg/ml or 700mg/ml SEMA3C recombinant protein, and then seeded on shaped Matrigel (50,000 cells/500ml medium per well).

Statistics

For each analysis, we examined at least three independent samples per experimental group. Results are expressed as mean ± SD relative to the specified controls. For all statistical analyses, we used a one-way ANOVA followed by a Tukey's test. P values of less than 0.05 were considered significant.

Optical Projection Tomography

Mice were paired in the evening, and the morning on which a vaginal plug was observed was defined as E0.5. Whole-mount E12.5 kidneys from the designated genotype were fixed in 4%PFA, permeabilised in 0.5% Triton X-100, and incubated overnight with anti-calbindin-D28K (Sigma Aldrich) in block (PBS/10% goat serum/0.1% Triton X-100). Kidneys were washed several times in PBS (1hr per wash) before overnight incubation with secondary Alexa Fluor antibodies at 4°C. Following several washes, kidneys were embedded in 1% low melting point agarose, dehydrated in methanol and cleared in a 1:2 mixture of benzyl alcohol and benzyl benzoate. Scanning was undertaken using a Bioptonics OPT Scanner 3001M (MRC Technology, Edinburgh, UK). NRecon software (Skyscan NV) was used for image reconstruction from projections using a back-projection algorithm. FIJI (Image J) was used for image analysis and 3D reconstruction.

Western Blotting

Proteins from kidney halves or quarters were extracted using RIPA lysis buffer supplemented with a cocktail of protease inhibitors. Total protein concentration was measured using a Bradford assay and equal amount of proteins (up to 50μg) were loaded on a NuPAGE 4-12% gradient gel (Invitrogen) and transferred to PVDF membrane (BioRad). A volume of urine containing 1μg of creatinine for each mouse sample was used. Primary antibodies were rabbit SEMA3C (Abcam), rabbit anti VE-Cadherin (Abcam), mouse anti-VEGFR2 (R&D systems), rabbit anti PLVAP, rabbit anti Occludin (Invitrogen) and abbit anti-GAPDH (Sigma). Blots were developed using ECL advance chemiluminescent reagent (GE Healthcare Life Sciences). Data were expressed as mean values ±SD of OD.

RNA extraction and Real-time analysis

Total RNA from kidney halves or quarters was extracted using TRIzol Reagent (Euromedex). RNA quality was checked by control of OD at 260 and 280 nm. cDNA was synthesized from 1 μg RNA using the Maxima First Strand cDNA Synthesis Kit (Thermo Fisher Scientific). Real-time PCR was performed with the Roche Light Cycler 480 detection system using SYBR green PCR master Mix (Roche Diagnostics). Specific primers for target mRNAs: *Gapdh* 5'-TGCGACTTCAACAGCAACTC-3' and 5'-CTTGCTCAGTGTCCTTGCTG-3', amplicon 200 bps; *Sema3c* 5' CCAGTGTGCACCTACCTGAA-3' and 5'-TCGGGTTGAAAGAGCATCGT-3' amplicon 103 bps; were used for amplification and a standard curve generated for each targeted transcripts. The unknown relative values were extrapolated from the standard curve and expression levels normalised to *Gapdh* expression. The average of triplicate reactions was used as a value of the sample.

Other standard methods with minor modifications were followed, which are detailed in Supplemental Material.

Results

Ectopic upregulation of SEMA3C upon kidney injury

In the embryonic kidney, *Sema3c* expression is detected in both early nephronic epithelium and ureteric bud- derived structures at E17.5 (black arrowhead and asterisk respectively, Figure 1A)[9], restricted to the papilla at birth (red arrowhead), and no longer detected in the adult. In the diseased kidney following surgically-induced (IR) and chemically-induced (FA) acute kidney injury, SEMA3C is ectopically upregulated compared to control kidneys and overexpression was detected as early as 5 hrs post injury (Figure 1B-C and Supplemental Figure 1A). SEMA3C was predominantly found in cortical tubules (white arrowheads, Figure 1C), in scattered tubular parts of the cortico-medulla region and in glomerular parietal epithelial cells (yellow arrowheads, Figure 1C). Quantification of tissue expression was performed in both IR- and FA-collected samples at different time points post injury, using RT-PCR and a previously validated set of primes[8] (Figure 1D-E). Increased serum urea, as an indicator of disrupted kidney function, confirms the efficiency of the IR and FA procedures (Figure 1D-E). Quantitation of *Sema3c* mRNA levels, normalised to Gapdh expression, confirmed the significant upregulation of *Sema3c* transcripts in the injured kidneys.

With the aim to translate this finding into clinical practice, tissue biopsies of adult patients with confirmed cases of Acute Tubular Necrosis (ATN) were also examined (Figure 2). SEMA3C was overexpressed in cases of transplanted kidneys diagnosed for ATN (ATN1), interstitial nephritis caused by drugs such as non-steroidal anti-inflammatory drugs (ATN2), vancomycin in HIV patients (ATN3) and immunoglobulin light chain amyloidosis and light chain deposition (ATN4). We concluded that SEMA3C upregulation was a conserved response to acute kidney injury both in mice and humans, although the timing of performing human biopsies differ for each patient and does not necessarily reflect the 48 hour time window post AKI of the current study.

De novo excretion and secretion of SEMA3C upon acute kidney injury

We next tested serum and urine samples of FA-treated mice for the presence of SEMA3C by Western Blot at the indicated time (Figure 2B). A 109 kDa SEMA3C recombinant protein (Sema3C rec., Figure 2B bottom) was used as a positive control. SEMA3C was detected in both urine and serum of FA-treated animals, but not in sham controls (Figure 2B). SEMA3C is cleaved, like other class III semaphorins, by furin-like endoproteases. Furin protein levels were reported to be low in blood[17, 18] while Furin proteolytic activity was increased in the urine post IR[19]. We also found that the 85 kDa full-length SEMA3C was also induced in the serum of FA-treated mice (Figure 2B, bottom).

SEMA3C receptors NRP1 and NRP2 are expressed in the renal vasculature during AKI progression

In addition to their well-documented expression in glomerular endothelial and mesangial cells[20, 21], we found that NRP1 and NRP2 expression colocalised with CD31-positive endothelial cells in peritubular capillaries surrounding the damaged tubules (yellow arrowhead, Figure 2C). We also observed some NRP1-positive, CD31-negative cells which were previously reported to be NG2-positive pericytes (red asterisk, Figure 2C and white arrowhead, Supplemental Figure 1B)[21]. The same expression pattern was observed for both NRP1 and NRP2 in IR-treated animals (data not shown). We found no expression of both NRP1 and NRP2 in kidney tubules, suggesting that SEMA3C is not involved in an autocrine loop of regulation. No double-positive NRP1-CD45 cells were observed in FA-treated kidneys (Supplemental Figure 1B), indicating that NRP1 does not seem to be expressed in leucocytes during kidney injury. We concluded that secreted SEMA3C from damaged tubules could potentially act in a paracrine faction on the kidney vasculature.

Genetic downregulation of Sema3c by conditional mutagenesis abrogates AKI-induced nephropathy

We next investigated the role of SEMA3C in the pathogenesis of AKI by deleting *Sema3c* in FA-treated mice. *Sema3c* conditional mutants (FA-*Sema3c* conds : *CAGGCre-ERTM;Sema3C*$^{flox/-}$) and wt littermate controls (FA-WT: *Sema3c*$^{flox/+}$ or *Sema3c*$^{flox/flox}$) were treated with Tamoxifen for 5 consecutive days (day 1 to 5) and subjected to a single intraperitoneal injection of FA (FA-treated animals) or vehicle (Sham animals) on day 8. Successful *Sema3C* deletion was demonstrated by recombination PCR, real-time PCR and by the reduction of SEMA3C induction upon FA treatment (Supplemental Figure 2). The analysis of Periodic Acid-Schiff (PAS)-stained kidney sections in FA-WT mice (*Sema3c*$^{flox/+}$ or *Sema3c*$^{flox/flox}$) showed characteristic features of ATN, including loss of brush border (black arrowhead), flattening of the renal tubular cells (red arrowheads) due to tubular dilatation (red asterisk) and intratubular cast formation (black arrows) compared to Sham mice (Figure 3A). These pathological changes and corresponding injury scores were significantly attenuated in FA-*Sema3c* conds (*CAGGCre-ERTM;Sema3C*$^{flox/-}$) as revealed by a reduced number of dilated tubules and by brush border maintenance in some tubular regions (Figure 3B). A significant diminution of serum urea levels is also observed in *Sema3c* conds compared to FA-WT mice, meaning that downregulation of *Sema3C* also ameliorated kidney function in AKI (Figure 3B). Of note, no changes in kidney function or injury were observed in vehicle-injected *Sema3c* conds (data not shown). We also found no significant SEMA3C ectopic upregulation in other organs such as the lungs, liver and heart, in neither the FA- nor the IR-induced AKI models (Supplemental Figure 3). Therefore, it is rather unlikely that in a 48hours timeframe, our analysis based on kidney injury reflects any other pathophysiological changes of extra-renal organs caused by *Sema3c* deletion in other organs. Because the degree of AKI-induced kidney injury correlates with neutrophil infiltration in mice and rats[22], we investigated neutrophil extravasation in our model and found a considerable reduction in renal neutrophil infiltration in *Sema3c* conditionals compared to FA-treated WT controls (Figure 3C top). Neutrophil extravasation greatly contributes to tubular

injury, and a significant drop in the apoptotic marker cleaved caspase 3 was detected in *Sema3c* conditionals compared to FA-treated animals 48 hrs post injury (Figure 3C, bottom).

SEMA3C does not sustain peritubular capillary loss during AKI

Because SEMA3C exerts potent inhibiting effects in cellular models of angiogenesis[23], we first hypothesised that by acting on NRP1- and NRP2-positive peritubular ECs, secreted SEMA3C could affect peritubular capillary density in the acutely damaged kidney. We used a similar approach and magnetically isolated peritubular ECs from wt kidneys as previously described (Figure 4A)[16]. When treated with increasing amounts of SEMA3C, purified ECs surprisingly increased their proliferative capacity as shown by a significant raise in ki67 positivity (Figure 4C, top), and underwent capillary-network formation on Matrigel in a dose-dependent manner (Figure 4C, bottom). *In vivo*, EC proliferation was only detected 48 hours post injury as previously described[24]. Indeed, some elongated cells double labelled for ki67 and CD34, indicative of EC origin, could be detected 48 hours post IR and FA-kidneys (yellow arrows, Figure 4C).

We next investigated the effect of *Sema3c* downregulation on peritubular vasculature *in vivo* using protein extracted from *sema3c* conditionals and wt littermates. Semi-quantitative expression of the EC marker VEGFR2 is significantly downregulated as early as 6 hrs post IR and also reduced 48 hours following FA injection (Figure 5B-B', C-C'). These observations are reminiscent of EC cell loss after AKI. However, when comparing *Sema3c* conditionals with their wildtype littermates, no significant difference in VEGFR2 expression was detected 48 hours post FA injection, indicating that SEMA3C might not participate in EC death during AKI (Figure 5C-C'). Furthermore, the expression of the adherens junction (AJ) VE-cadherin presented a drastic reduction 48 hours post FA injection, while no significant discrepancy between *Sema3c* conditionals and wildtype mice (Figure 5C-C') could be observed. Such a result implies that SEMA3C does not sustain EC death but rather triggers another pathophysiological alteration in AKI.

Considering that VE-cadherin is closely related to EC contacts and vascular permeability, we also analysed the expression of other molecules involving capillary permeability: the EC plasmalemma vesicle-associated protein PLVAP that specifically localises to diaphragms of fenestrae in fenestrated capillaries and participates in transcellular permeability. Although the PLVAP expression seems stable in sham animals, we observed a very dynamic regulation of this protein in the diseased kidney irrespective of the mouse genotype and regardless of EC death (Figure 5C-C'). These results suggest that EC passage through cytoplasmic fenestrae is highly regulated in the diseased kidney, with no significant changes between *Sema3c* conditionals and wt mice. Finally, we tested the tight junction (TJ) epithelial adhesion molecule Occludin. We found Occludin expression downregulated in FA-treated wt kidneys and upregulated in *Sema3c* conditional protein extracts (Figure 5C-C'). In regard to the large amount of epithelial cell death observed in AKI, Occludin change in expression is more likely to reflect the amount of tubular injury, which is less pronounced in *Sema3c* conditionals compared to wt littermates (Figure 3), than a modulation in TJ associated permeability.

Sema3c downregulation decreases kidney vascular permeability leading to tissue oedema and improves post-injury microvascular renal blood flow in AKI

Increased vascular permeability leading to tissue oedema was observed as early as 6 hours post IR in the mouse[25]. 24 hours post unilateral IR, the L/R kidney ratio had significantly increased (Figure 6A). Likewise, kidney to body weight ratio following 24 hrs of FA treatment had dramatically risen compared to control sham kidneys (Figure 6A). These results suggest that in addition to tubular dilatation, a substantial infiltration of fluid in the renal parenchyma could have occurred. Remarkably, the kidney to body weight ratio was significantly lower in FA-treated *Sema3c* conditionals compared to FA-treated WT controls (Figure 6A), suggesting that downregulation of *Sema3c* might be able to reduce tissue oedema in the FA-induced AKI nephropathy. A non-significant drop in L/R kidney ratio was also observed in IR-*Sema3c* conditionals compared to IR-

treated WT controls (Figure 6A). However, when we used a more sensitive method that consists in measuring Evans Blue dye (EB) extravasation in the left ischemic kidney following unilateral IR (Figure 6B), we found that disrupting SEMA3C signalling was also able to reduce vascular permeability in IR (Figure 6B). Results showed that vascular permeability has (i) increased 24hours post reperfusion in the ischemic kidney and (ii) significantly dropped in IR-*Sema3c* conditionals. Interstitial oedema participates in the diminished microvascular flow and alters oxygen diffusion observed in AKI pathologies. Microangiographies performed with high molecular weight dextran (FITC-Dextran (2000 kDa)) on sham animals revealed that normal vascular blood flow allows FITC-Dextran to be dispatched throughout the kidney and highlight peritubular capillaries and glomeruli of control sham mice (Figure 6C). However, only very scattered vascular regions of the kidneys were positive for FITC-Dextran in FA-CTR 10mins post injection, implying severe microvascular leakage and hypoperfusion (Figure 6C). Conversely, significantly more kidney vascular regions were stained for FITC-Dextran in FA-*Sema3c* conditionals (Figure 6A). Our results suggest that downregulation of *Sema3c* is able to induce a diminution in interstitial oedema and an improvement of renal blood flow.

SEMA3C is a vascular permeability factor

To determine whether SEMA3C could directly increase blood vessel permeability, we used two distinct procedures. Intradermal injections of both VEGF-A and SEMA3A, which are key inducers of vascular permeability[26], caused increased extravasation of EB dye into the tissue compared to PBS (Figure 7). Similarly, SEMA3C was able to induce a significant increased vascular leakage of the EB dye, establishing a novel function for SEMA3C as a vascular permeability factor (Figure 7). To test whether SEMA3C induced vascular permeability in kidneys, we next used intravital microscopy and retro-orbital injection of VEGF-A or SEMA3C combined with tracer FITC-Albumin. In this experiment, we monitored the presence of green tubular casts, which represents the rapid passage, via a permeability signal, of the usually unfiltered FITC-Albumin. As expected,

we did not find any casts in mice receiving FITC-Albumin alone over 30mins post injection (Figure 8 and Supplemental Movie 1). However, we observed a drastic effect on glomerular vascular permeability when we injected 5μg of VEGF-A (Figure 8A and Supplemental Movie 2). The first cast was observed as early as 12 mins post injection and was followed by a quick dynamic of cast formation and excretion, indicative of the powerful permeability effect of VEGF-A on kidney vasculature (Supplemental Movie 2). When mice were injected with 5μg of SEMA3C, the first cast was observed at around 23 mins (Figure 8A, Supplemental Movie 3) and 4 out of 8 treated mice presented with tubules filled with FITC-Albumin at 30 mins post injection. At 35mins, 7 out of 8 injected mice had accumulated FITC-Albumin in their kidney tubules (Figure 8B). A similar dynamic of cast formation was observed when VEGF-A concentration was lowered to 2μg (Supplemental movie 4). We also examined peritubular capillary branches which correspond to the reported sites of EB dye extravasation in pathological conditions[27]. Interestingly, in both VEGF-A and SEMA3C injected mice, we observed the accumulation of FITC-Albumin at the capillary intersections and to a lesser extent, along the longitudinal axed of the microvessels in VEGF-A (red arrowhead Figure 8A). Overall, our data provide evidence for a novel SEMA3C function as a vascular permeability factor acting on the peripheral and internal vasculature.

Discussion

By taking advantage of a repertoire of *in vivo* and *ex vivo* techniques, we have characterised the function of the class III semaphorin SEMA3C in the context of AKI. First, we found that SEMA3C was ectopically expressed; de novo secreted and excreted in acutely damaged kidneys. Second, we found that *Sema3c* conditional deletion ameliorated tissue injury and renal function in AKI-induced nephropathy, central to our hypothesis of a causative role for SEMA3C-driven pathways in kidney disease. Third, we identified an undocumented role for SEMA3C in promoting vascular permeability. We demonstrated that mice lacking *Sema3c* presented with reduced interstitial oedema and neutrophil infiltration and improved renal blood flow. Our combined analysis provides an improved mechanistic understanding of the disease and the description of a novel deleterious tubulovascular cross-talk during AKI progression.

In this study, we demonstrated that the ectopic upregulation of SEMA3C in AKI is critical in the progression of the disease. Our analysis established that downregulation of *Sema3c* was able to reduce kidney injury, kidney neutrophil infiltration and associated apoptosis as well as ameliorate kidney functions in FA-induced nephropathy. Neutrophils are the first cell types recruited to sites of inflammation[28], where they not only aggravates renal tissue damage but also leads to increased vascular permeability[29-31]. Our observed changes in vascular permeability likely contribute to extravasation and worsened renal damage.

Considering the central role played by semaphorins and neuropilins in angiogenesis, it was essential to test whether SEMA3C could interfere with normal EC functions in AKI. Our findings using magnetically sorted ECs from the peritubular vasculature are in agreement with previous conclusions on the proangiogenic role of SEMA3C in glomerular ECs [7], and show that kidney ECs, whether of glomerular or peritubular origins, react the same way to SEMA3C stimulation. However, very little EC proliferation occurs within the first 48 hours following kidney injury, suggesting that SEMA3C pro-angiogenic function has no functional contribution to the acute phase.

In contrast, a drastic reduction of endothelial markers VEGFR2 and VE-cadherin was observed, indicating significant EC death and consistent with previous reports [4]. However, the fact that no significant difference was detected between wildtype and *Sema3c* conditionals further eliminated the possibility that SEMA3C aggravates renal tissue injury via effecting on EC quantity in the acute phase of AKI. Therefore, the dysfunction of the existing endothelium might be an alternative pathway induced by SEMA3C.

Now that the EC quantity did not change, and that S3C must play its [ACalmont1]deleterious role via NRP1 on ECs, we turned our attention to the dysfunction of existing ECs. [ACalmont2][AC3]

We next tested the possibility that SEMA3C could modify renal microvascular permeability, as previously reported for SEMA3A and SEMA3C receptor NRP1 [32, 33]. We first showed that SEMA3C was able to induce vascular permeability of dermal and kidney ECs, which is, to our knowledge, the first evidence of a direct role for this semaphorin in modulating vascular permeability *in vivo*. In this context, we also found that SEMA3C pro-permeable capacity was as powerful as the one described for SEMA3A. These comparable results are of importance as SEMA3A role in permeability was reported to be the key detrimental event involved in ischemia-induced brain tissue damage [26] and in the loss of endothelial barrier integrity in glioblastoma [34]. We further showed that a downregulation of SEMA3C was able to (i) reduce EB dye vascular leakage through peritubular ECs in unilateral IR-induced nephropathy and (ii) ameliorate microvascular blood flow in FA-induced nephropathy. Our results are in agreement with previous studies showing that in pathophysiological conditions, renal microvascular hyperpermeability contributes to an overall decline in GFR through interstitial oedema, increased tubular pressure and tubular obstruction [35]. Moreover, while both the tubuloglomerular feedback and the imbalance of vasomotor factors contribute to renal vasoconstriction [4], the consequent altered vascular tone exacerbates vascular leakage [36]. Taken together, our data suggest that SEMA3C deleterious functions operate through the regulation of microvascular permeability in the acutely damaged kidney, while efforts to attenuate vascular leakage through inhibiting αvβ5 integrin showed significant protective effects in IR[37].

We further investigated the mechanism by which SEMA3C could increase vascular permeability. The finding that SEMA3C could inhibit AJ integrity through VE-Cadherin endocytosis in 30 mins[23] strongly suggests that AJ modulation is an essential mechanism in our model. In addition and in agreement with this hypothesis, SEMA3C receptor NRP1 activation leads to the phosphorylation and subsequent internalisation of VE-cadherin to open AJs and increased vascular permeability[38], which exerts no influence on EC quantity but on its activity. Indeed, we observed both (i) a rapid tissue response to SEMA3C permeability signal *in vivo* and (ii) no significant difference in Ve-Cadherin expression between wildtype mouse and *Sema3c* conditionals. Our findings not only support the previous studies[23, 38], but have further revealed that the internalised VE-cadherin was not degraded and might be stored and recycled. However, we also tested additional permeability pathways such as transcellular pathway marked by PLVAP and TJ molecule Occludin and found no significant modulation.

Finally and in regards to the large amount of interstitial fluid accumulation and neutrophil infiltration, we cannot eliminate a possible effect on renal lymphatic vasculature. Indeed, the inactivation of SEMA3E/Plexin-D1 pathway could ameliorate cardiac function in a mouse model of acute cardiac injury by promoting reactive lymphangiogenesis to alleviate oedema, remove inflammatory factors and regulate the immune reaction[39]. Considering that SEMA3C is also capable of interacting with Plexin-D1[40] and inhibiting lymphangiogenesis[41], SEMA3C downregulation might mitigate renal tissue injury via increasing lymphangiogenesis, which could also involve NRP2[42].

The thorough study of tissue-specific *Nrp1* and *Nrp2* mouse mutants could be informative to carefully dissect the essential contribution of NRP-driven pathways in AKI. However, the fact that NRP1 binds both VEGF-A and class III semaphorins [12] and that NRP2 can sometimes compensate for the loss of NRP1 [8] adds to the level of complexity. An interesting study reported that when a specific NRP1 blocking peptide directed to class III semaphorin SEMA3A was used in IR-induced AKI[43], it was able to reduce tubular injury, blunt tubular cell apoptosis and attenuate renal

dysfunction. However, the vascular contribution to AKI was not investigated by the authors. Nevertheless, the combined SEMA3C-SEMA3A analyses score the importance of the deleterious Class III semaphorins-NRP1 axis in AKI progression and offer options for therapeutic strategies. In particular, specific compounds directed to the NRP1-class III semaphorin binding site could possibly reduce tissue oedema without compromising NRP1-VEGF-A-dependant vessel growth and renal microvasculature maintenance.

Finally, we found that SEMA3C was *de novo* excreted and secreted in FA-induced injury and that SEMA3C urinary levels raise significantly and well before urea levels elevate in the serum of FA-treated mice. In that respect, further investigations in human patients should investigate whether SEMA3C could serve as an early marker of AKI and/or a predictive marker of AKI to CKD progression. Even though it would be difficult to determine the exact initial time of AKI patients in clinical practice, unlike that of mouse AKI models, such a molecule present early after kidney injury might have significant translational potential.

In summary, our data indicate that SEMA3C is produced by damaged tubular cells during AKI and suggests that it is a key detrimental mediator of renal injury. Our study is supported by recent single cell RNAseq analysis showing *Sema3c* upregulation in novel epithelial-to-stromal crosstalks following AKI[44]. Furthermore, AKI to CKD transition is associated with an increase S*ema3c* expression[45]. Our analysis embraces the complexity of signalling events that promote AKI progression and emphasises the role of vascular permeability as an important underlying cause of the disease. In that sense, our study provides an improved mechanistic understanding of the disease and the first evidence for the role of SEMA3C in kidney disease. Finally, our result might inform a number of areas of current research, in particular the ones studying SEMA3C and cancer progression whereby vessel permeability is also known to facilitate the metastatic spread of cancer[46].

Authors Contributions

ACai, GY, SP, PF, BS, RK, MG and AC conducted the experiments and acquired data. XDYC provided human samples. AC designed the research study. SP and PF helped design the intravital permeability assay. CChatziantoniou, PJS and AC provided the funding. ACai and AC wrote the manuscript with contributions from all the authors.

Acknowledgements

We thank Fabiola Terzi for helpful discussions and are grateful to Sonja Djudjaj, Michael Goligorsky, Mark Lipphardt, Aoife Waters, David Long and Elisavet Vasilopoulou for technical advice with Mile's assay, peritubular capillary insolation and FA-induced nephropathy model. We thank the staff at INSERM UMRS 1155 and at UCL Great Ormond Street-Institute of Child Health for help with mouse husbandry.

Disclosure

None

Funding

This study was supported by the INSERM and Sorbonne University, two National Academy of Medicine fellowships to ACai and GY, an ANR grant [19-CE14-0011-01] to CC, a British Heart Foundation grant [RG/15/13/28570] to PJS, a Marie Curie Personal Fellowship [704450, Horizon2020] to AC and a BAYER Grants4Targets [ID 2017-08-2159] to AC.

References

1. Mehta RL, Cerdá J, Burdmann EA, et al. International Society of Nephrology's 0by25 initiative for acute kidney injury (zero preventable deaths by 2025): a human rights case for nephrology. *Lancet*. Jun 27 2015;385(9987):2616-43. doi:10.1016/s0140-6736(15)60126-x
2. Guzzi F, Cirillo L, Roperto RM, Romagnani P, Lazzeri E. Molecular Mechanisms of the Acute Kidney Injury to Chronic Kidney Disease Transition: An Updated View. *International journal of molecular sciences*. Oct 6 2019;20(19)doi:10.3390/ijms20194941
3. Verma SK, Molitoris BA. Renal endothelial injury and microvascular dysfunction in acute kidney injury. *Semin Nephrol*. Jan 2015;35(1):96-107. doi:10.1016/j.semnephrol.2015.01.010
4. Basile DP, Anderson MD, Sutton TA. Pathophysiology of acute kidney injury. *Comprehensive Physiology*. Apr 2012;2(2):1303-53. doi:10.1002/cphy.c110041
5. Cai A, Chatziantoniou C, Calmont A. Vascular Permeability: Regulation Pathways and Role in Kidney Diseases. *Nephron*. 2021;145(3):297-310. doi:10.1159/000514314
6. He Z, Tessier-Lavigne M. Neuropilin is a receptor for the axonal chemorepellent Semaphorin III. *Cell*. Aug 22 1997;90(4):739-51.
7. Banu N, Teichman J, Dunlap-Brown M, Villegas G, Tufro A. Semaphorin 3C regulates endothelial cell function by increasing integrin activity. *FASEB journal : official publication of the Federation of American Societies for Experimental Biology*. Oct 2006;20(12):2150-2. doi:10.1096/fj.05-5698fje
8. Plein A, Calmont A, Fantin A, et al. Neural crest-derived SEMA3C activates endothelial NRP1 for cardiac outflow tract septation. *J Clin Invest*. Jul 1 2015;125(7):2661-76. doi:10.1172/jci79668
9. Reidy K, Tufro A. Semaphorins in kidney development and disease: modulators of ureteric bud branching, vascular morphogenesis, and podocyte-endothelial crosstalk. *Pediatr Nephrol*. Sep 2011;26(9):1407-12. doi:10.1007/s00467-011-1769-1
10. Cole-Healy Z, Vergani P, Hunter K, Brown NJ, Reed MW, Staton CA. The relationship between semaphorin 3C and microvessel density in the progression of breast and oral neoplasia. *Experimental and molecular pathology*. Aug 2015;99(1):19-24. doi:10.1016/j.yexmp.2015.03.041
11. Binch AL, Cole AA, Breakwell LM, et al. Class 3 semaphorins expression and association with innervation and angiogenesis within the degenerate human intervertebral disc. *Oncotarget*. Jul 30 2015;6(21):18338-54. doi:10.18632/oncotarget.4274
12. Schwarz Q, Ruhrberg C. Neuropilin, you gotta let me know: should I stay or should I go? *Cell Adh Migr*. Jan-Mar 2010;4(1):61-6.
13. Chau YY, Brownstein D, Mjoseng H, et al. Acute multiple organ failure in adult mice deleted for the developmental regulator Wt1. *PLoS Genet*. Dec 2011;7(12):e1002404. doi:10.1371/journal.pgen.1002404
14. Le Clef N, Verhulst A, D'Haese PC, Vervaet BA. Unilateral Renal Ischemia-Reperfusion as a Robust Model for Acute to Chronic Kidney Injury in Mice. *PLoS One*. 2016;11(3):e0152153. doi:10.1371/journal.pone.0152153
15. Long DA, Woolf AS, Suda T, Yuan HT. Increased renal angiopoietin-1 expression in folic acid-induced nephrotoxicity in mice. *J Am Soc Nephrol*. Dec 2001;12(12):2721-31.
16. Kida Y, Zullo JA, Goligorsky MS. Endothelial sirtuin 1 inactivation enhances capillary rarefaction and fibrosis following kidney injury through Notch activation. *Biochemical and biophysical research communications*. Sep 23 2016;478(3):1074-9. doi:10.1016/j.bbrc.2016.08.066
17. Huffman AM, Rezq S, Basnet J, Yanes Cardozo LL, Romero DG. SARS-CoV-2 Viral Entry Proteins in Hyperandrogenemic Female Mice: Implications for Women with PCOS and COVID-19. *International journal of molecular sciences*. Apr 25 2021;22(9)doi:10.3390/ijms22094472
18. Khoury EE, Knaney Y, Fokra A, et al. Pulmonary, cardiac and renal distribution of ACE2, furin, TMPRSS2 and ADAM17 in rats with heart failure: Potential implication for COVID-19 disease. *Journal of cellular and molecular medicine*. Apr 2021;25(8):3840-3855. doi:10.1111/jcmm.16310

19. Jayakumar C, Ranganathan P, Devarajan P, Krawczeski CD, Looney S, Ramesh G. Semaphorin 3A is a new early diagnostic biomarker of experimental and pediatric acute kidney injury. *PLoS One*. 2013;8(3):e58446. doi:10.1371/journal.pone.0058446
20. Bartlett CS, Scott RP, Carota IA, et al. Glomerular mesangial cell recruitment and function require the co-receptor neuropilin-1. *Am J Physiol Renal Physiol*. Dec 1 2017;313(6):F1232-f1242. doi:10.1152/ajprenal.00311.2017
21. Wnuk M, Anderegg MA, Graber WA, Buergy R, Fuster DG, Djonov V. Neuropilin1 regulates glomerular function and basement membrane composition through pericytes in the mouse kidney. *Kidney Int.* Apr 2017;91(4):868-879. doi:10.1016/j.kint.2016.10.010
22. Okusa MD, Linden J, Huang L, Rieger JM, Macdonald TL, Huynh LP. A(2A) adenosine receptor-mediated inhibition of renal injury and neutrophil adhesion. *Am J Physiol Renal Physiol*. Nov 2000;279(5):F809-18. doi:10.1152/ajprenal.2000.279.5.F809
23. Yang WJ, Hu J, Uemura A, Tetzlaff F, Augustin HG, Fischer A. Semaphorin-3C signals through Neuropilin-1 and PlexinD1 receptors to inhibit pathological angiogenesis. *EMBO Mol Med*. Jul 20 2015;7(10):1267-84. doi:10.15252/emmm.201404922
24. Long DA, Price KL, Ioffe E, et al. Angiopoietin-1 therapy enhances fibrosis and inflammation following folic acid-induced acute renal injury. *Kidney Int*. Aug 2008;74(3):300-9. doi:10.1038/ki.2008.179
25. Awad AS, Ye H, Huang L, et al. Selective sphingosine 1-phosphate 1 receptor activation reduces ischemia-reperfusion injury in mouse kidney. *Am J Physiol Renal Physiol*. Jun 2006;290(6):F1516-24. doi:10.1152/ajprenal.00311.2005
26. Hou ST, Nilchi L, Li X, et al. Semaphorin3A elevates vascular permeability and contributes to cerebral ischemia-induced brain damage. *Scientific reports*. Jan 20 2015;5:7890. doi:10.1038/srep07890
27. Babickova J, Klinkhammer BM, Buhl EM, et al. Regardless of etiology, progressive renal disease causes ultrastructural and functional alterations of peritubular capillaries. *Kidney Int*. Jan 2017;91(1):70-85. doi:10.1016/j.kint.2016.07.038
28. Li L, Huang L, Sung SS, et al. The chemokine receptors CCR2 and CX3CR1 mediate monocyte/macrophage trafficking in kidney ischemia-reperfusion injury. *Kidney Int*. Dec 2008;74(12):1526-37. doi:10.1038/ki.2008.500
29. Awad AS, Rouse M, Huang L, et al. Compartmentalization of neutrophils in the kidney and lung following acute ischemic kidney injury. *Kidney Int*. Apr 2009;75(7):689-98. doi:10.1038/ki.2008.648
30. Kelly KJ, Williams WW, Jr., Colvin RB, et al. Intercellular adhesion molecule-1-deficient mice are protected against ischemic renal injury. *J Clin Invest*. Feb 15 1996;97(4):1056-63. doi:10.1172/jci118498
31. Li L, Huang L, Vergis AL, et al. IL-17 produced by neutrophils regulates IFN-gamma-mediated neutrophil migration in mouse kidney ischemia-reperfusion injury. *J Clin Invest*. Jan 2010;120(1):331-42. doi:10.1172/jci38702
32. Cerani A, Tetreault N, Menard C, et al. Neuron-derived semaphorin 3A is an early inducer of vascular permeability in diabetic retinopathy via neuropilin-1. *Cell metabolism*. Oct 1 2013;18(4):505-18. doi:10.1016/j.cmet.2013.09.003
33. Roth L, Prahst C, Ruckdeschel T, et al. Neuropilin-1 mediates vascular permeability independently of vascular endothelial growth factor receptor-2 activation. *Science signaling*. Apr 26 2016;9(425):ra42. doi:10.1126/scisignal.aad3812
34. Treps L, Edmond S, Harford-Wright E, et al. Extracellular vesicle-transported Semaphorin3A promotes vascular permeability in glioblastoma. *Oncogene*. May 19 2016;35(20):2615-23. doi:10.1038/onc.2015.317
35. Sutton TA. Alteration of microvascular permeability in acute kidney injury. *Microvascular research*. Jan 2009;77(1):4-7. doi:10.1016/j.mvr.2008.09.004

36. Orsenigo F, Giampietro C, Ferrari A, et al. Phosphorylation of VE-cadherin is modulated by haemodynamic forces and contributes to the regulation of vascular permeability in vivo. *Nature communications*. 2012;3:1208. doi:10.1038/ncomms2199
37. McCurley A, Alimperti S, Campos-Bilderback SB, et al. Inhibition of αvβ5 Integrin Attenuates Vascular Permeability and Protects against Renal Ischemia-Reperfusion Injury. *Journal of the American Society of Nephrology : JASN*. Jun 2017;28(6):1741-1752. doi:10.1681/asn.2016020200
38. Acevedo LM, Barillas S, Weis SM, Göthert JR, Cheresh DA. Semaphorin 3A suppresses VEGF-mediated angiogenesis yet acts as a vascular permeability factor. *Blood*. Mar 1 2008;111(5):2674-80. doi:10.1182/blood-2007-08-110205
39. Maruyama K, Naemura K, Arima Y, et al. Semaphorin3E-PlexinD1 signaling in coronary artery and lymphatic vessel development with clinical implications in myocardial recovery. *iScience*. Apr 23 2021;24(4):102305. doi:10.1016/j.isci.2021.102305
40. Gitler AD, Lu MM, Epstein JA. PlexinD1 and semaphorin signaling are required in endothelial cells for cardiovascular development. *Dev Cell*. Jul 2004;7(1):107-16. doi:10.1016/j.devcel.2004.06.002
41. Mumblat Y, Kessler O, Ilan N, Neufeld G. Full-Length Semaphorin-3C Is an Inhibitor of Tumor Lymphangiogenesis and Metastasis. *Cancer research*. Jun 1 2015;75(11):2177-86. doi:10.1158/0008-5472.can-14-2464
42. Yuan L, Moyon D, Pardanaud L, et al. Abnormal lymphatic vessel development in neuropilin 2 mutant mice. *Development*. Oct 2002;129(20):4797-806.
43. Ranganathan P, Jayakumar C, Mohamed R, Weintraub NL, Ramesh G. Semaphorin 3A inactivation suppresses ischemia-reperfusion-induced inflammation and acute kidney injury. *Am J Physiol Renal Physiol*. Jul 15 2014;307(2):F183-94. doi:10.1152/ajprenal.00177.2014
44. Rudman-Melnick V, Adam M, Potter A, et al. Single-Cell Profiling of AKI in a Murine Model Reveals Novel Transcriptional Signatures, Profibrotic Phenotype, and Epithelial-to-Stromal Crosstalk. *J Am Soc Nephrol*. Dec 2020;31(12):2793-2814. doi:10.1681/asn.2020010052
45. Harzandi A, Lee S, Bidkhori G, et al. Acute kidney injury leading to CKD is associated with a persistence of metabolic dysfunction and hypertriglyceridemia. *iScience*. Feb 19 2021;24(2):102046. doi:10.1016/j.isci.2021.102046
46. Harney AS, Arwert EN, Entenberg D, et al. Real-Time Imaging Reveals Local, Transient Vascular Permeability, and Tumor Cell Intravasation Stimulated by TIE2hi Macrophage-Derived VEGFA. *Cancer discovery*. Sep 2015;5(9):932-43. doi:10.1158/2159-8290.cd-15-0012

Figures with FigureLegends

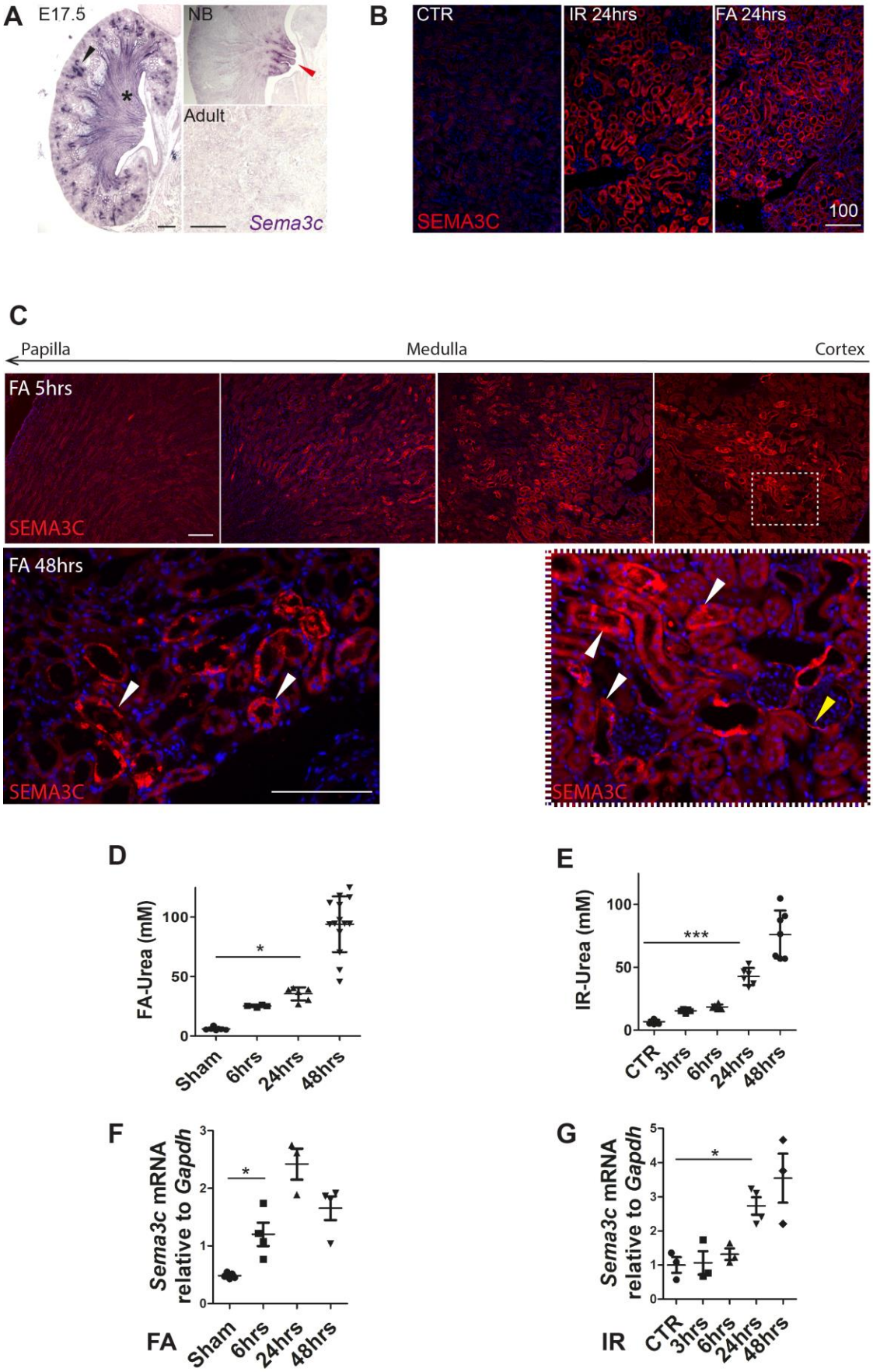

Figure 1. ***Ectopic upregulatin of SEMA3C in two well-characterised mouse models of AKI.*** **(A)** *Sema3c* in situ hybridisation on E17.5newborn (NB) and adult wild-type (wt) mouse kidneys. Black arrowhead and asterisk indicate nephronic epithelium and ureteric bud-derived structures respectively; red arrowhead indicates the renal papilla. **(B)** SEMA3C immunostaining on kidneys 24 hrs post IR or FA injury (n=3). **(C)** Serial kidney sections of mice immunostained for SEMA3C at 5 or 48 hrs post FA injury at the papilla, medulla and cortex levels (n=3). The boxed area is shown at higher magnification. White and yellow arrowheads indicate SEMA3C upregulation in proximal tubules and in glomerular parietal epithelial cells respectively. **(D, E)** Serum urea levels in FA- and IR-AKI model. **(F, G)** Quantification of renal *Sema3c* mRNA expression levels relative to *Gapdh* in FA- and IR-AKI model. $*P \leq 0.05$, $***P \leq 0.001$. Scale bar: 100 µm

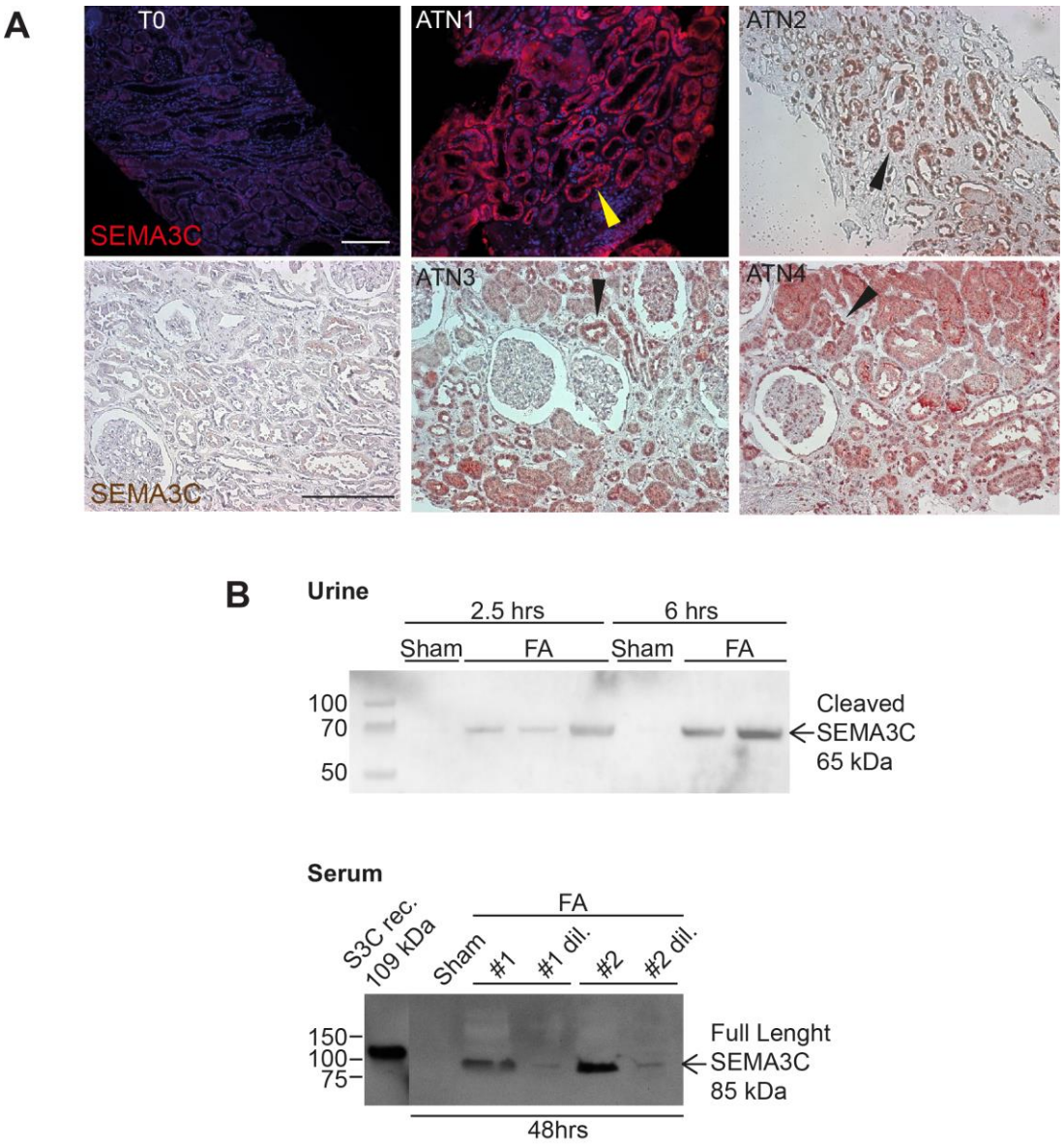
A
T0
SEMA3C
ATN1
ATN2
ATN3
ATN4
SEMA3C
B
Urine
2.5 hrs
6 hrs
Sham
FA
Sham
FA
100
70
50
Cleaved
SEMA3C
65 kDa
Serum
FA
S3C rec.
109 kDa
Sham
#1
#1 dil.
#2
#2 dil.
150
100
75
Full Lenght
SEMA3C
85 kDa
48hrs
C
FA 24hrs
NRP1
NRP2
CD31
CD31
NRP1CD31
NRP2CD31

Figure 2. SEMA3C *ectopic upregulation in human biopsies, de novo excretion and secretion of SEMA3C upon mouse kidney injury.*

(A) SEMA3C immunostaining of time-zero control (T0) and acute tubular necrosis (ATN) patient tissue biopsies. ATN1, kidney transplant patient diagnosed with ATN. ATN2, nonsteroidal anti-inflammatory drug-induced ATN. ATN3, renal amyloidosis derived from IgA-delta deposition. ATN4, vancomycin and acyclovir-induced ATN. **(B)** Top: representative western blot image of cleaved SEMA3C isoform excretion in mouse urine at 2.5 hrs (n=3) or at 6 hrs (n=3) after FA or Sham injections. Bottom: representative western blot image of full-length SEMA3C secretion in mouse serum 48 hrs post FA injection (n=2). #1 dil. and #2 dil. represent a 20 times dilution of sample #1 and #2 respectively. S3C rec. represents SEMA3C 109 kDa recombinant protein. **(C)** Kidneys were immunolabelled for NRP1 or NRP2 and endothelial marker CD31 24 hrs post FA injection. Yellow arrowheads indicate NRP1/CD31 (left) or NRP2/CD31 (right) double-positive peritubular ECs; red asterisk indicates NRP1 positive, CD31 negative pericytes. Scale bar: 100 µm.

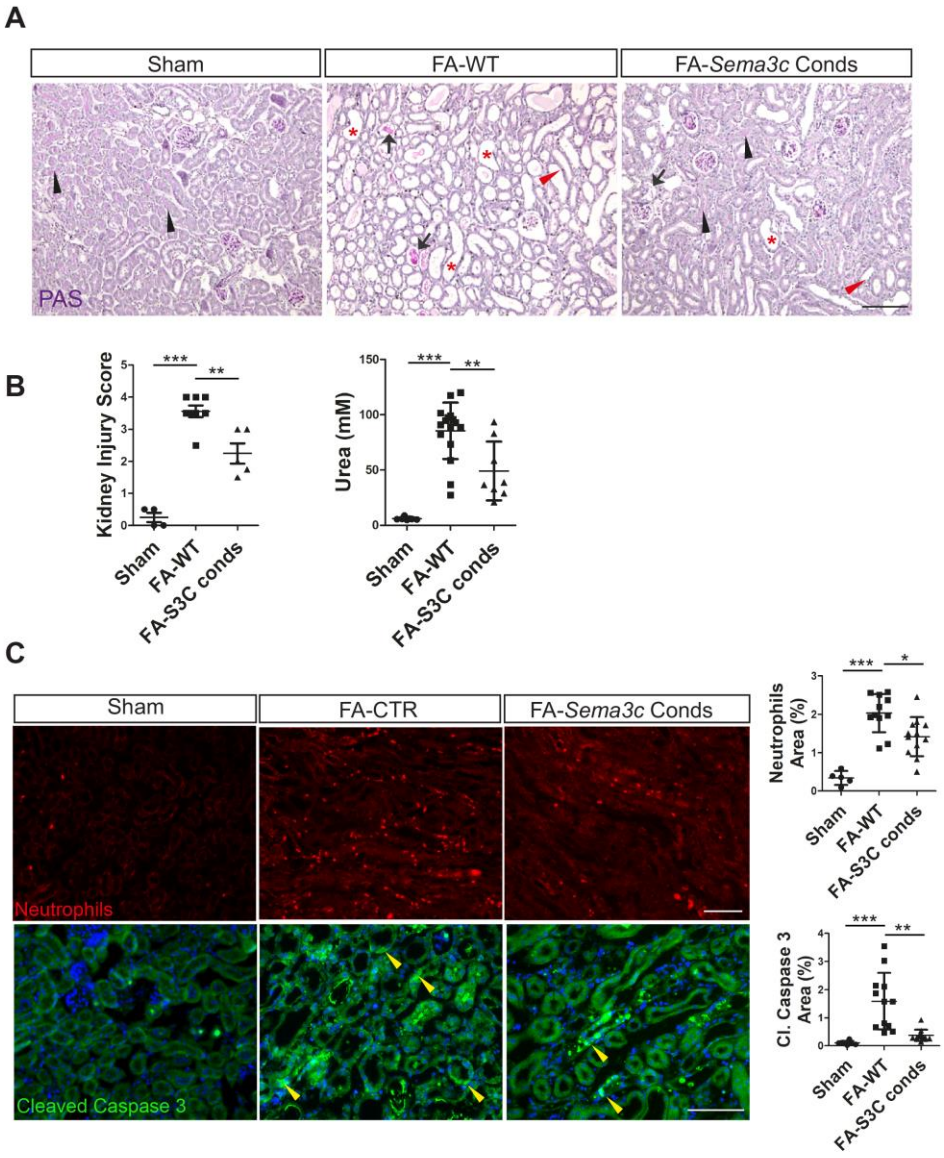

Figure 3. ***Genetic downregulation of Sema3c by conditional mutagenesis abrogates AKI-induced nephropathy***

(A, B) PAS-stained sections of Sham, wildtype (FA-WT) and *Sema3c* conds (FA-S3C conds) mouse kidneys at 48 hrs post FA injection **(A)** with corresponding quantification of serum urea and kidney injury score **(B)** (n≥5). Black arrowheads indicate loss of brush border; red arrowheads indicate flattening of renal tubular cells; red asterisks indicate tubular dilatation; black arrows indicate intratubular cast formation. **(C)** Sections of Sham, FA-WT and FA-S3C conds mouse kidneys were immunolabelled with anti-neutrophil antibody (red) or for the apoptotic marker cleaved caspase 3 (green). Corresponding staining were quantified (% area relative to DAPI-positive cells) (n=4). *P<0.05, **P ≤ 0.01, ***P ≤ 0.001. Yellow arrowheads indicate apoptotic renal tubular cells. Scale bar: 100 µm **(A),** 50 µm **(C)**.

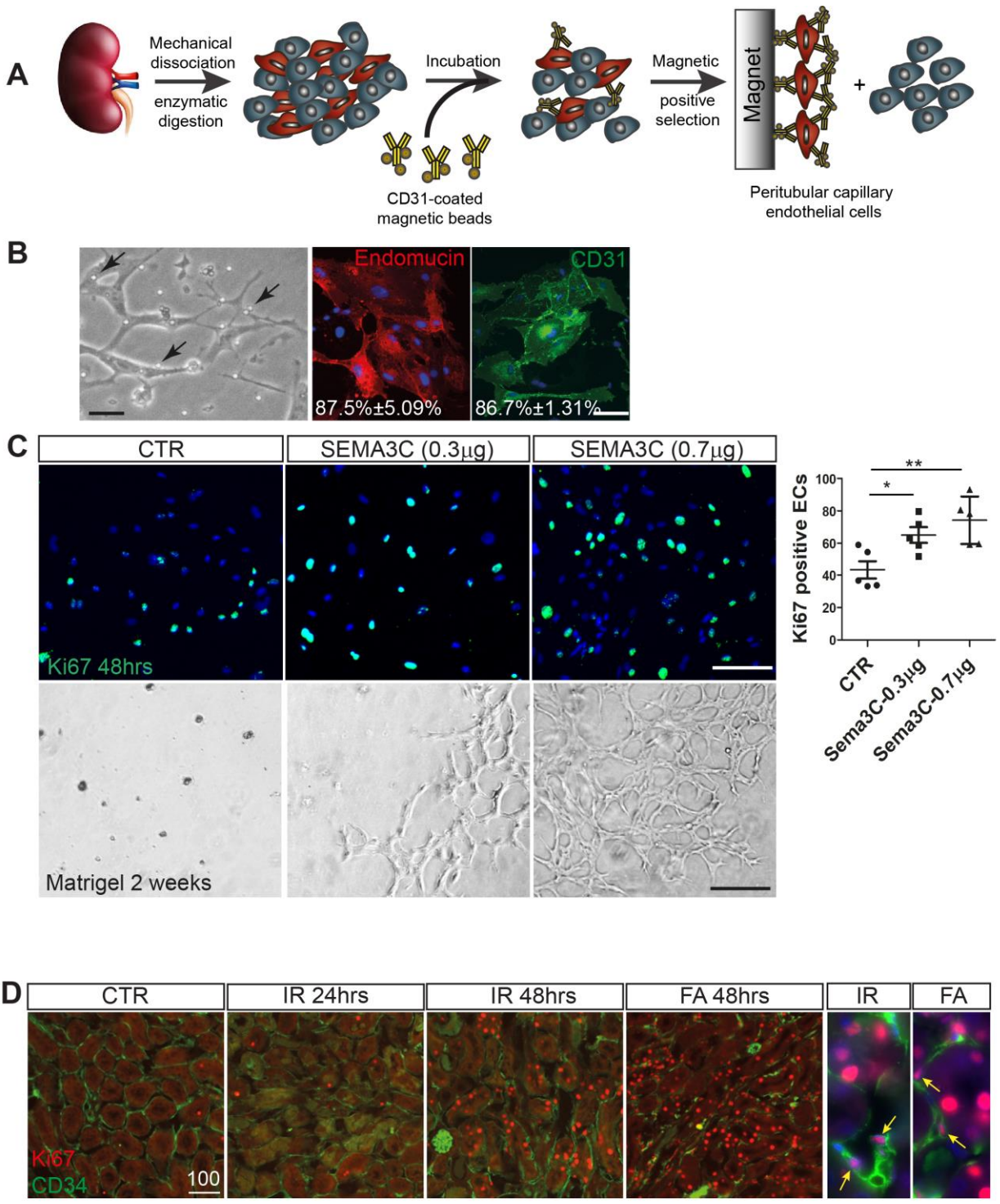

Figure 4. ***SEMA3C SEMA3C does not sustain peritubular capillary loss during AKI.***

(A) Schematic procedure of magnetic isolation of adult mouse peritubular ECs. **(B)** Left: phase contrast image of isolated peritubular ECs, black arrows indicate magnetic beads conjugated with CD31 antibodies. Right: primary ECs stained with Endomucin and CD31. Indicated numbers means % of positivity for each marker (performed on two sets of isolation). **(C)** Isolated primary ECs were cultured with 0 (CTR), 0.3 and 0.7µg of recombinant SEMA3C for either 48 hrs and stained for Ki67 (n=5 per condition, upper) or seeded on Matrigel and cultured for 2 weeks (n≥3 per

condition, lower). **(D)** Ki67 and CD34 double-staining of kidneys 24 hours or 48 hours post FA- and IR-induced nephropathies. Yellow arrows indicate Ki67/CD34 double-positive ECs (n=3). *P<0.05, **P ≤ 0.01. Scale bars: 20µm **(B)**, 50µm **(C)**, 100 µm **(D)**.

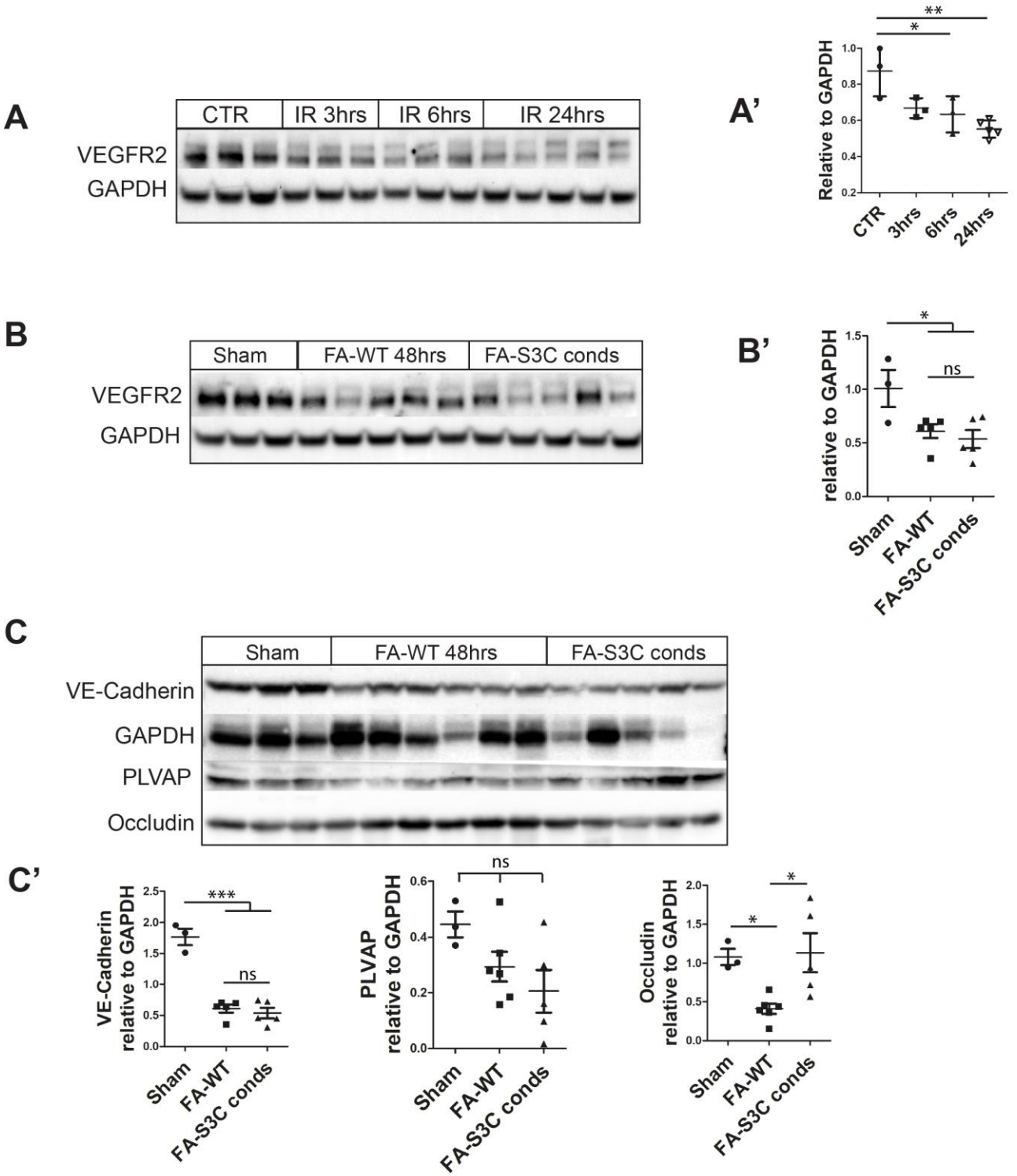

Figure 5.

(A) Western blot analysis of EC marker VEGFR2 at different time points (3, 6 and 24 hours) post IR-induced kidney injury. **(B)** Western blot analysis of EC marker VEGFR2 at 48 hrs post FA-induced kidney injury in wildtype mouse and *Sema3c* conditionals. **(C)** Western blot analysis of endothelial adhesion molecule VE-cadherin, EC plasmalemma vesicle-associated protein PLVAP and TJ molecule Occludin at 48 hrs post FA-induced kidney injury in wildtype mouse and *Sema3c*

conditionals. **(A'-C')** Corresponding quantification (n≥3) of **(A-C).** *P<0.05, **P<0.01, ***P ≤ 0.001. ns: not significant.

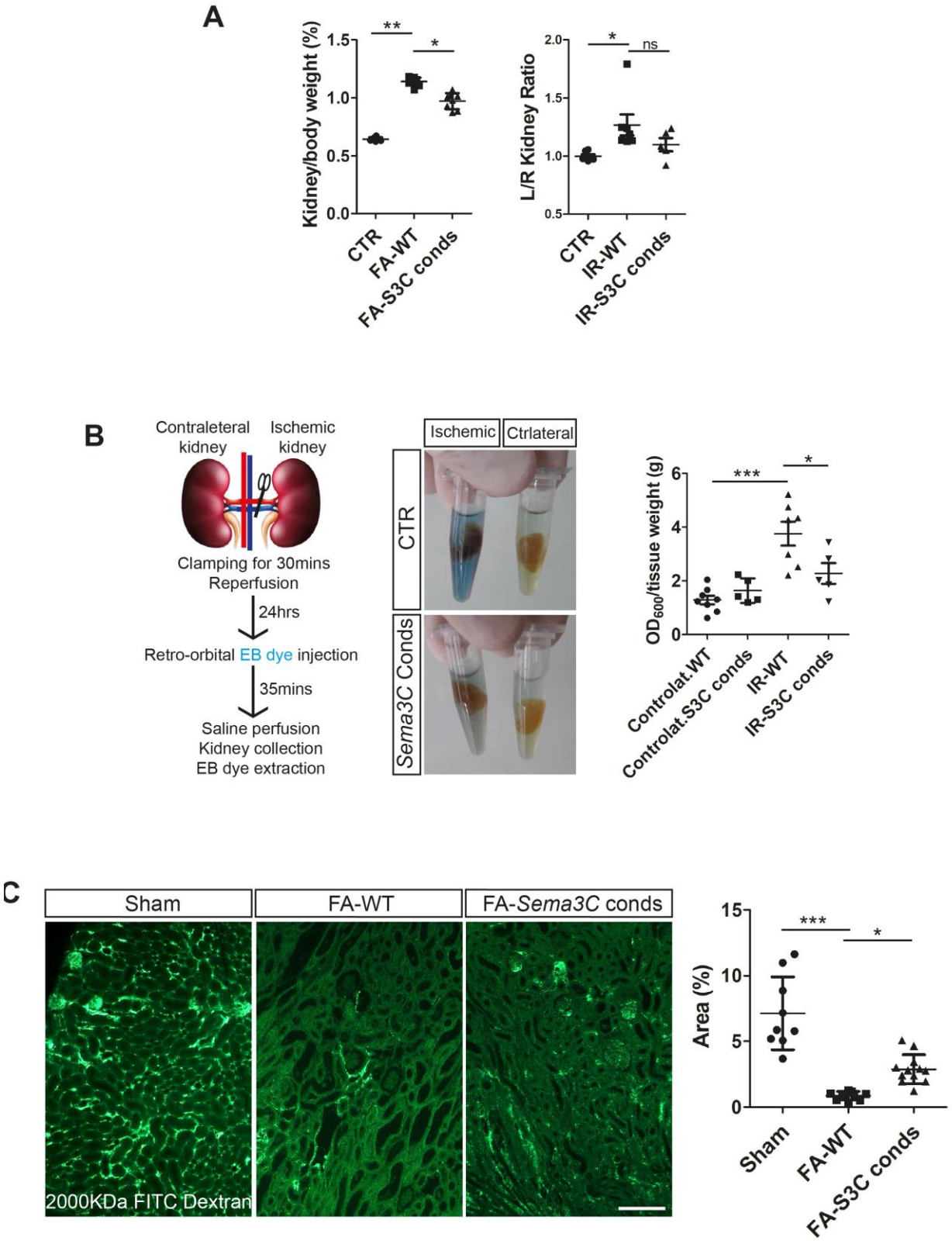

Figure 6. ***Sema3c downregulation ameliorates microvascular blood flow and decreases kidney vascular permeability leading to tissue oedema in AKI.***

(A) Kidney/bodyweight ratios of FA-treated animals at the indicated genotype (left) or left/right kidney ratios of IR-treated animals at the indicated genotypes (right) were quantified (n>3). **(B)** Schematic procedure of a modified Mile's assay performed 24 hours following unilateral IR in mice (left). EB dye extravasation from peritubular capillaries of the left ischemic kidney is photographed and compared to contralateral kidney in both controls and *Sema3c* conditionals (middle). Quantification of EB dye extravasation is presented as OD_{600} per 10^{-3} Kg of tissue weight for contralateral kidneys, IR-treated left kidneys and IR-treated left kidneys from *Sema3c* conditionals (right). (n≥5). **(C)** 2000 kDa FITC-Dextran was intravenously injected into Shams, FA-treated controls and FA-treated *Sema3c* conditionals to evaluate microvascular blood flow 10mins post injection. FITC-Dextran positive areas were quantified. *P≤ 0.05, ***P≤ 0.001. Ctrlateral: contralateral. (n=3). Scale bars: 100 μm **(C**

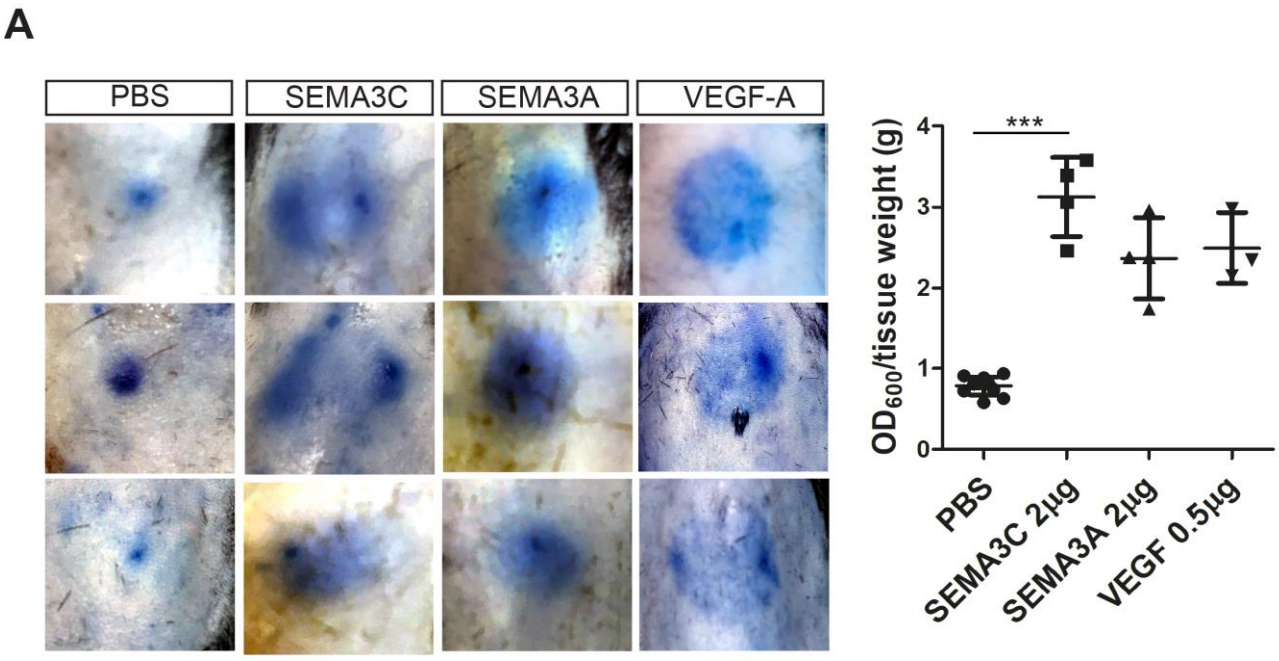

Figure 7. ***SEMA3C is a vascular permeability factor of the peripheral (skin) vasculature.***

Representative images of Mile's assays performed on shaved dorsal skin of wildtype mice. 50µl intradermal punctures were realised with PBS, SEMA3C (2µg), SEMA3A (2µg), or VEGF-A (0.5µg); EB dye extravasation was quantified 30mins post injection. Results are expressed as OD_{600} per 10^{-3} kg of tissue weight (n=4). ***P≤ 0.001

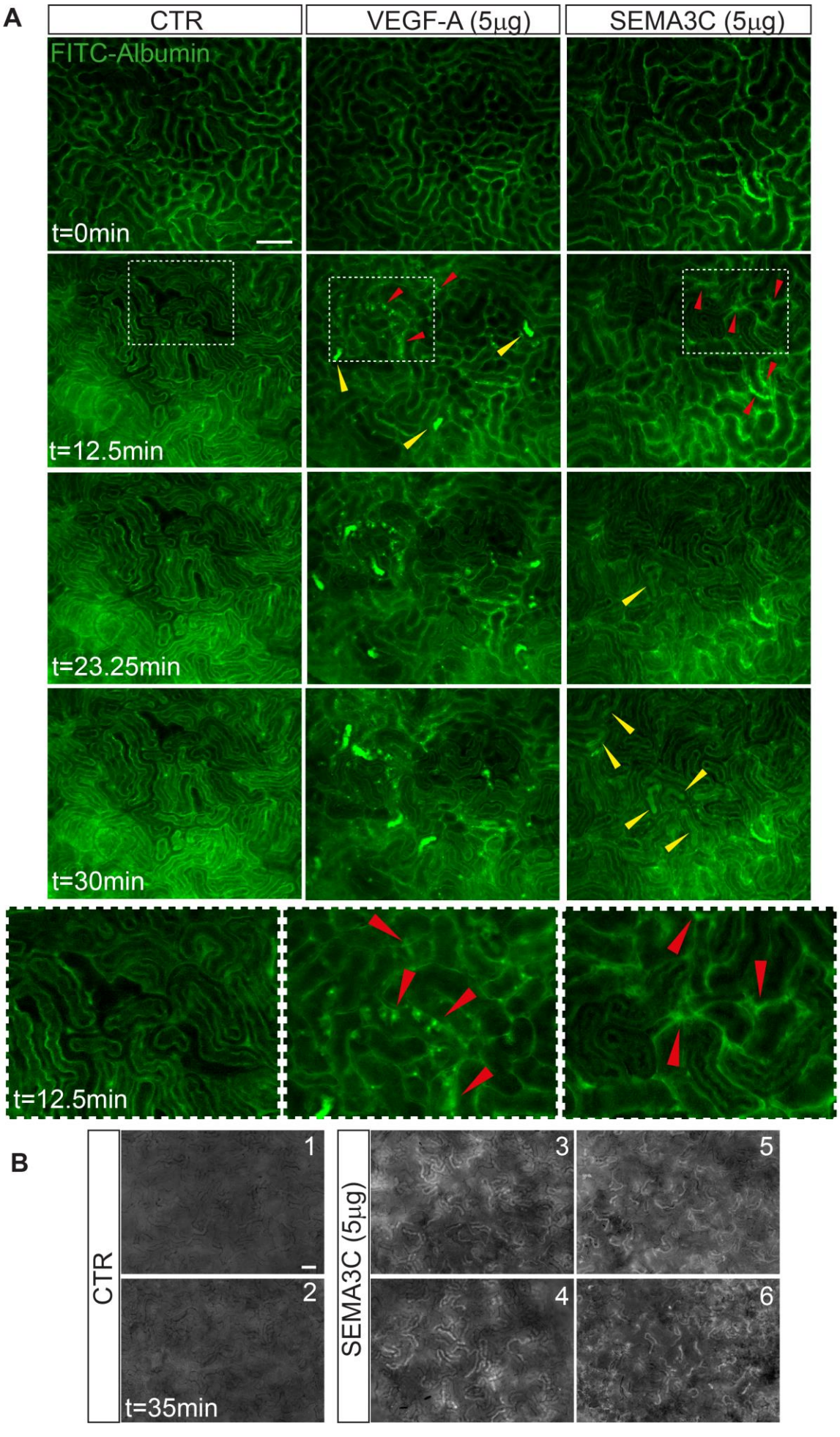
A
CTR
VEGF-A (5μg)
SEMA3C (5μg)
FITC-Albumin
t=0min
t=12.5min
t=23.25min
t=30min
t=12.5min
B
CTR
SEMA3C (5μg)
1
2
3
4
5
6
t=35min

Figure 8. ***SEMA3C is a vascular permeability factor of the internal (renal) vasculature.***

(A) Representative intravital microscopy images of mouse kidneys acquired at the indicated time post retro-orbital injection of FITC-Albumin mixed with either 0.9% NaCl (control, CTR) (n=5), 5µg VEGF-A (n=3), or 5µg SEMA3C (n=8). Yellow arrowheads indicate the presence of FITC-Albumin positive casts in VEGF-A and SEMA3C injected mice. **(B)** Tilling acquisition performed 35mins post retro-orbital injection of FITC-Albumin mixed with either 0.9% NaCl (control, CTR) (n=5) or 5µg SEMA3C (n=8). Scale bars: 100 µm

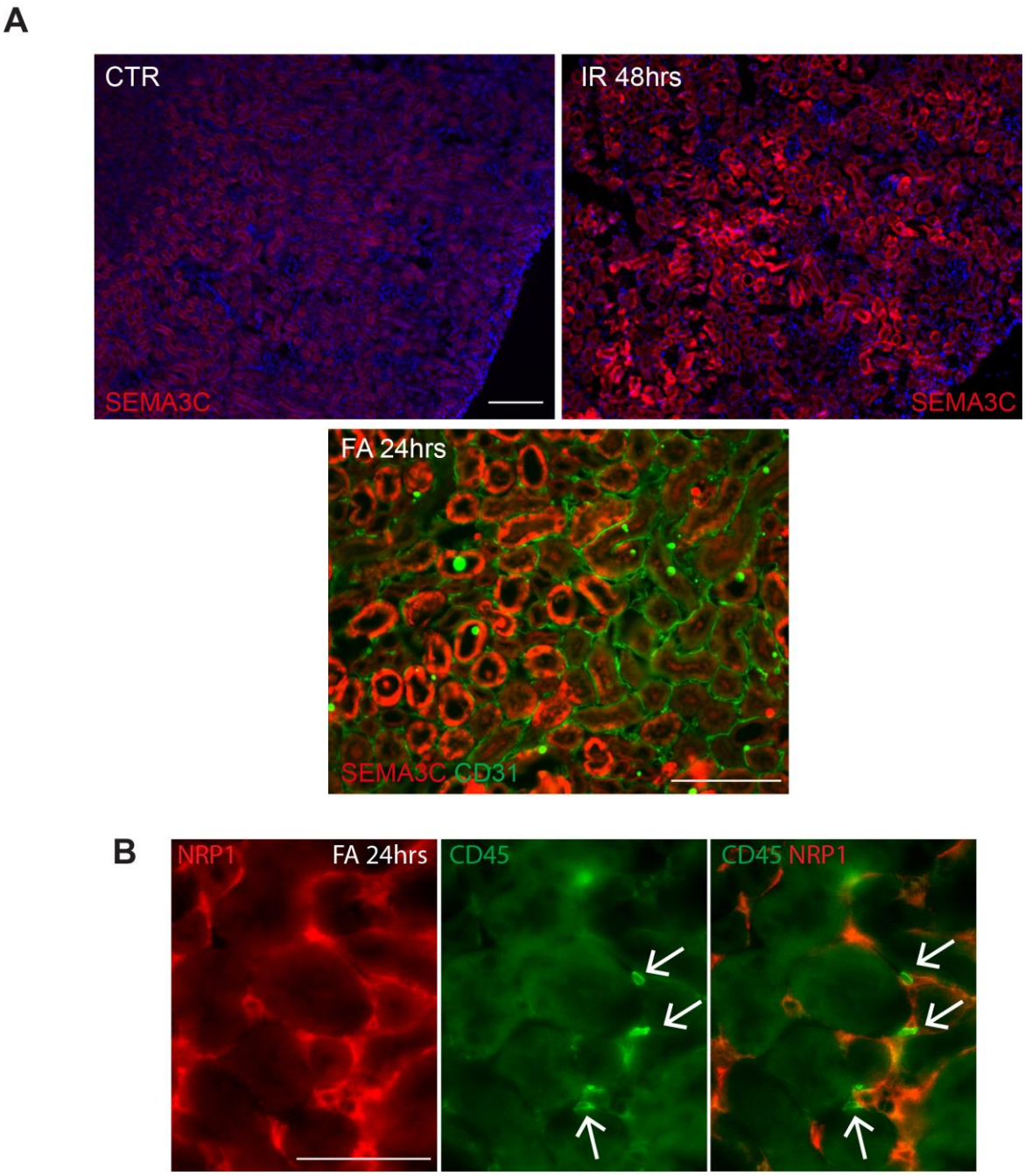

Supplemental Figure 1.

(A) Kidneys were immunolabelled for SEMA3C 48 hrs post IR (top, right) or SEMA3C (red) and CD31 (green) colocalisation 24 hrs FA injury (bottom) (n=3). **(B)** Kidneys were immunolabelled for NRP1 (red) and inflammatory cell marker CD45 (green) 24 hrs post FA injection. Scale bar: 100 µm (A, B).

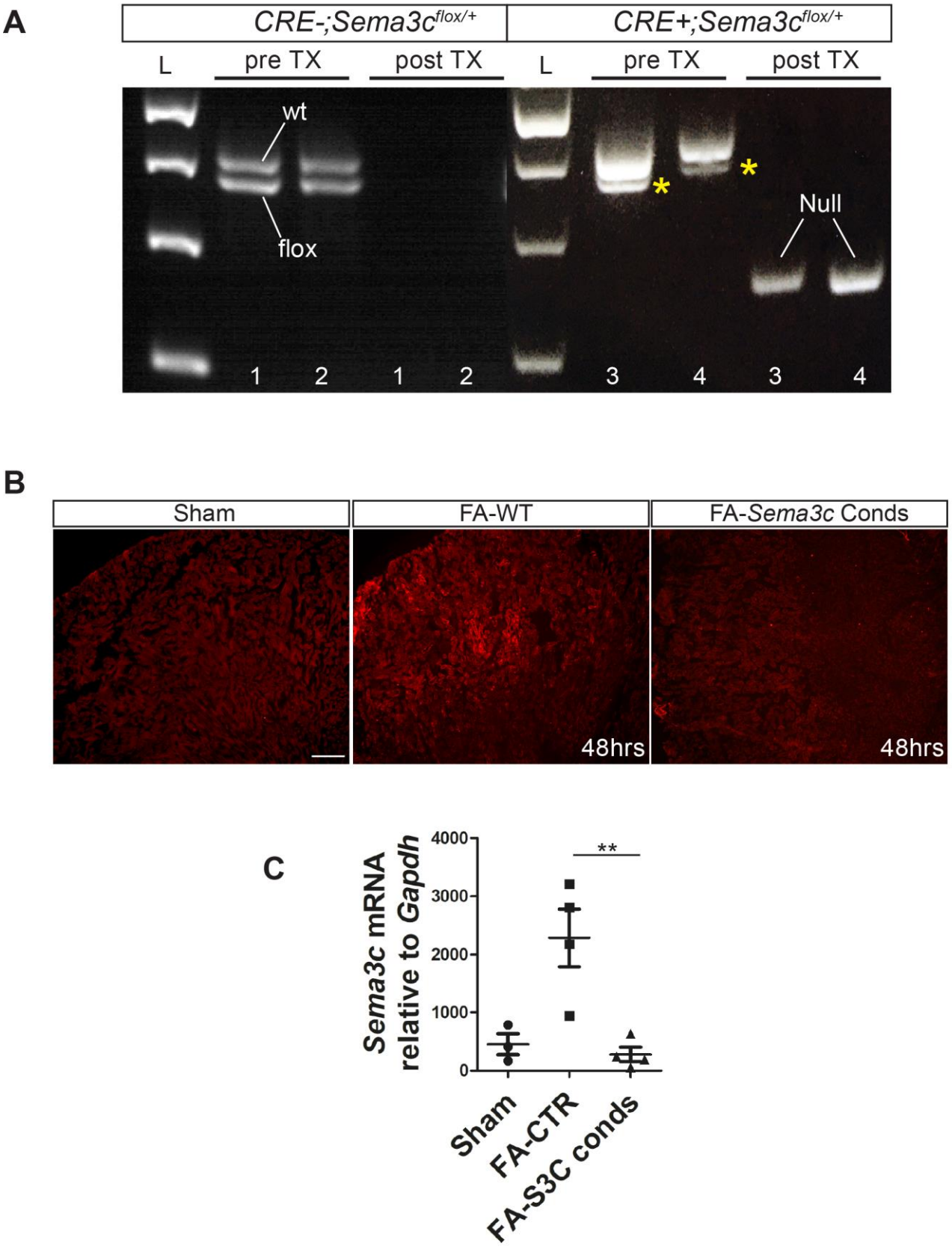

Supplemental Figure 2. ***Sema3c conditional strategy***

(A) PCRs were performed with two sets of primers on *Sema3c* conditional hetz (Cre^{+}; $Sema3C^{flox/+}$) mouse tails and *Sema3c* null allele ($Sema3C^{-/+}$) ~~primer was applied~~ to univocally evaluate $Sema3C^{flox/+}$ recombination. Without CRE, no $Sema3C^{-/+}$ allele was detected for sample 1 and 2

post Tamoxifen (TX) injection. Conversely, in Cre^{+}; $Sema3C^{flox/+}$ mice number 3 and 4, recombination of Sema3c flox allele is visible (yellow asterisk) and de novo *Sema3C*$^{-/+}$ allele is produced post TX injection. **(B)** Kidney sections of Sham, FA-treated WT and FA-treated *Sema3c* conditional mice stained for SEMA3C. SEMA3C upregulation upon FA treatment is blunt in *Sema3c* conditionals. Scale bar: 200 µm.

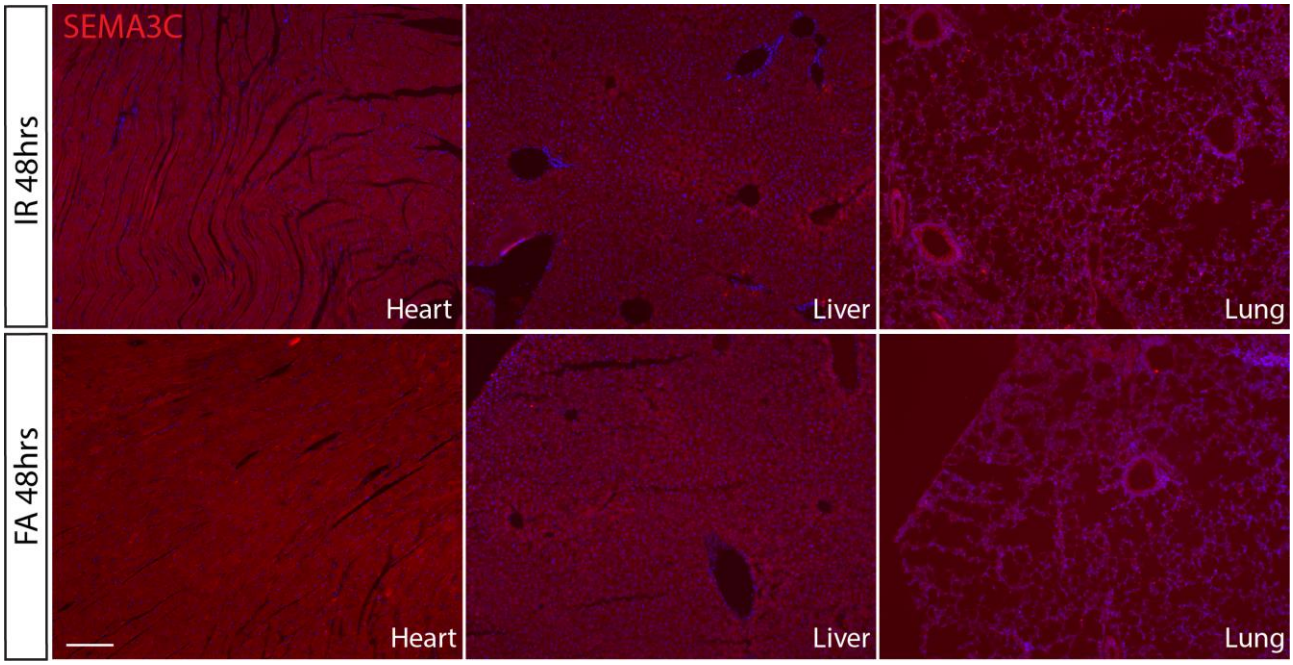

Supplemental Figure 3. ***SEMA3C upregulation is not detected in extra-renal tissues.***

Sections of hearts, livers and lungs 48 hrs post IR injury or FA injection immunostained for SEMA3C (n=3). Scale bar: 100 µm.

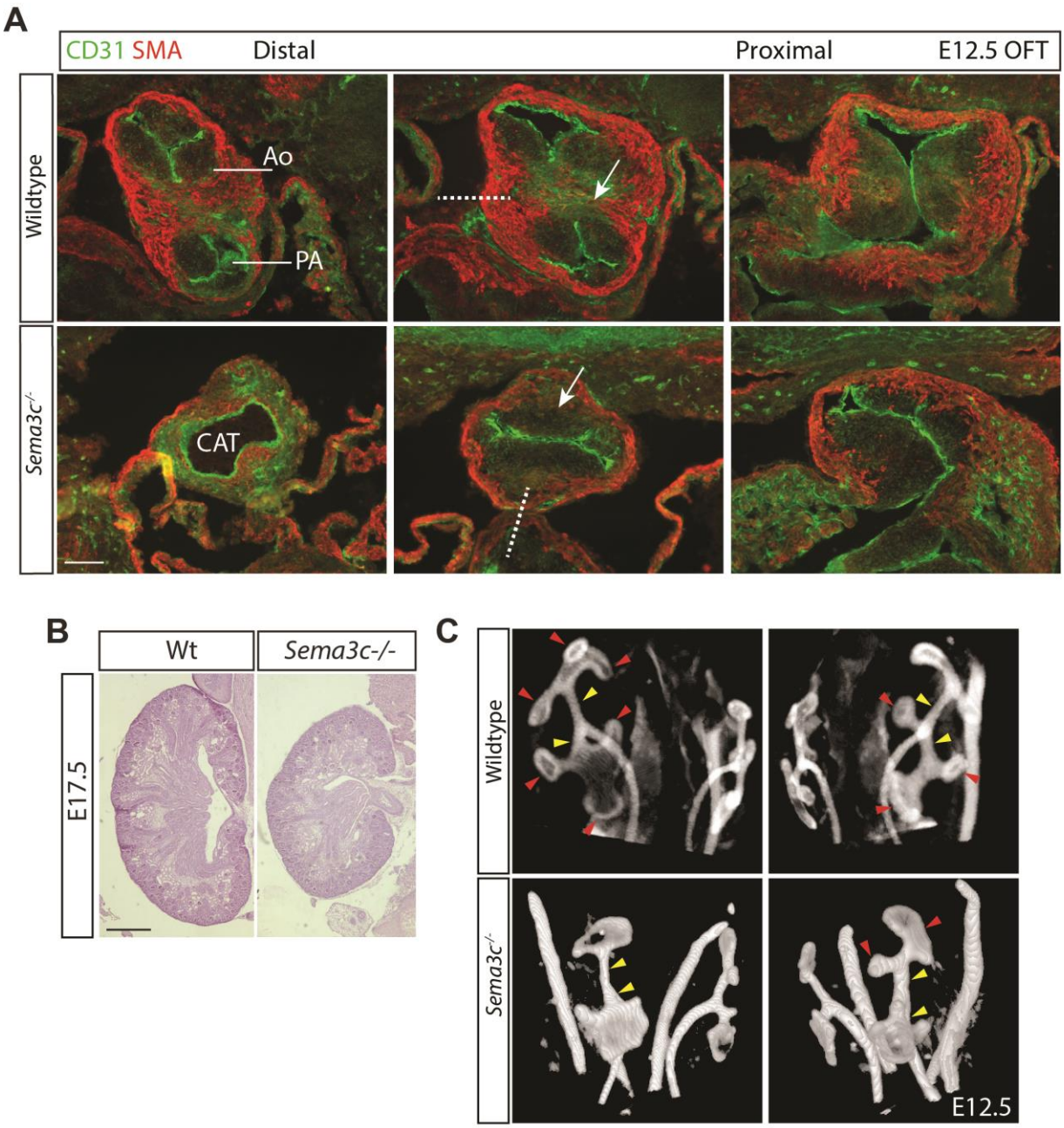

Supplemental Figure 4. ***Sema3c*$^{-/-}$** ***embryos display cardiac and renal defects.***

(A) Serial sections of wt and *Sema3c*$^{-/-}$ (n=3) E12.5 OFTs at proximal, medial, and distal levels were immunolabeled for CD31 and myocyte marker SMA. Arrows indicate septal bridge myocardialisation; dotted lines indicate the axis of septal bridge formation. Ao, aorta; PA, pulmonary artery; CAT, common arterial trunk.: **(B)** Sections of wt and smaller *Sema3c*$^{-/-}$ E17.5 kidneys were hematoxylin and eosin-stained. **(C)** Three-dimensional reconstruction of OPT (Optical Projection Tomography) acquisitions of wt and *Sema3c*$^{-/-}$ E12.5 kidneys stained with anti-calbindin. First (yellow arrows) and second (red arrows) branching of the ureteric bud are shown. Decreased ureteric bud branching is observed at E12.5 in *Sema3c*$^{-/-}$ embryos. Scale bar: 100 µm.